Dr Fatih Güleç[1,*]
Dr Emir Hüseyin Şimşek[2,*]
Hilal Tanıker Sarı[2]

Prediction of biomass pyrolysis mechanisms and kinetics – Application of Kalman filter

Abstract

In order to predict the pyrolysis mechanisms of four different biomasses (Asbos-Psilocaulon utile, Kraalbos-Galenia africane, Scholtzbos-Pteronia pallens, and Palm shell) were investigated by a novel method called Kalman filter and the results compared with the regression analysis. Both analyses were applied to five different generalised biomass pyrolysis models consisting of parallel and series irreversible-reversible reaction steps. The models consisting of reversible reactions in addition to parallel pyrolysis steps demonstrated a better fit with the experimental results. The pyrolysis step from biomass $\rightarrow$ bio-oil has the highest reaction rates ($3.9*10^{-3}$, $8.2*10^{-3}$, $9.3*10^{-3}$, and $13.5*10^{-3}$ min^{-1}) compared with the other pyrolysis steps defined in the models. Kalman filter is, therefore, defined as one of the promising filtering and prediction methods for the estimation of detailed pyrolysis mechanisms and model parameters using minimum experimental data.

Key Words: Biomass, Kalman filter, Pyrolysis, Pyrolysis models, Regression analysis.

[1] Chemical Engineering, Faculty of Engineering, University of Nottingham, Nottingham, NG7 2RD, UK
[2] Chemical Engineering, Faculty of Engineering, Ankara University, 06100 Ankara, Turkey
**Corresponding Authors: Fatih.Gulec1@nottingham.ac.uk, Gulec.Fatih@outlook.com, Emir.Simsek@eng.ankara.edu.tr*

1. Introduction

Biomass feedstocks are defined as clean, environmentally friendly, and inexpensive energy sources [1, 2]. Additionally, biomass feedstocks are also considered CO_2 neutral energy sources since they are an integral part of the global carbon cycle [3, 4]. The biomasses are therefore one of the most promising feedstocks for the production of clean energy and fine chemicals using thermal (pyrolysis, combustion, hydrothermal) and biological process pathways [5-7]. However, there are several obstacles to the full fill the commercialisation of bioenergy and bioproducts via these technologies, which include the resourcing of biomass, ineffective biomass refinery technologies, a lack of cost-competitive bioproducts and a limited and/or unstable supply of biofuels and bioproducts. Furthermore, the differences in chemical and biological structures of biomass resources increase the obstacles to the commercialisation of these technologies. Pyrolysis is one of the commonly used processes in which the biomasses can be effectively converted into more valuable and clean products; gas, liquid (bio-oil) and solid (bio-char) [8-10]. In the pyrolysis process, the chemical bonds in hemicellulose, cellulose and lignin structures of biomasses are thermally degraded in an oxygen-free environment. The pyrolysis process is usually categorised into three groups as "slow pyrolysis", "fast pyrolysis" and "flash pyrolysis" based on heating rate, temperature, and residence time of process conditions. To maximise the bio-char yield, a lower temperature (~400 °C) with a slower heating rate for a longer residence time (days) was suggested [11]. To maximise the gas yield, a higher temperature (650-1000 °C) with a higher heating rate for a shorter residence time (<1s), and finally, to maximise the liquid yield, an intermediate temperature (425-600 °C) with a higher heating rate (1000-10000 °C/s) for a shorter residence time (<3s) were suggested [11]. Identifying the fundamental of biomass pyrolysis mechanisms is, therefore, a challenge due to the differences in pyrolysis conditions and biomass structures.

Isoconversional methods also called model-free methods are the most popular methods for the kinetic analysis of biomass pyrolysis, which determined the activation energy using the thermogravimetric analysis data [12, 13]. In those methods, the reaction model is the same at a specific conversion whatever may be the heating rate [13]. Furthermore, the reaction rate (degradation rate) can be determined by considering its temperature dependence according to Arrhenius law. To identify the pyrolysis mechanism, the single-step global kinetic model "biomass → volatile gases + char" was proposed as an irreversible first-order pyrolysis mechanism, which is one of the widely used models [14-16]. However, the single-step global model has limitations to predict the whole pyrolysis mechanisms due to the consideration of only primary reaction mechanisms [9]. As pyrolysis reaction mechanisms could also include secondary reactions such as bio-oil degradation to gas or polymerisation of bio-oils to bio-char [17, 18]. Therefore, the pyrolysis reaction was modified with additional secondary interactions; as the primary reaction runs through with parallel reactions "virgin biomass → volatile + gas and virgin biomass → char" and the products in the primary reactions give second interactions as " $(\text{volatile} + \text{gas})_1 + (\text{char})_1 \rightarrow (\text{volatile} + \text{gas})_2 + (\text{char})_2$" [19, 20]. After demonstrating the importance of secondary reactions, the studies on detailed lumped kinetic models have been getting more attention [21, 22]. Cuoci et al. [22] suggested lumped kinetic models for the biomass devolatilization and investigate the kinetics for each type of biomass structures of hemicellulose, cellulose, and lignin with 15 reactions under 30 lumped species. Additionally, a detailed mechanistic study was also investigated for the devolatilization and gas-phase reaction of the gases released through the thermal decomposition of biomass-based on three reference components by Ranzi et al. [21] to describe the biomass pyrolysis mechanism.

Although understanding the reaction mechanisms is of utmost importance for the process optimisation and reactor design, the measurement techniques fall short of all the variables in this kind of dynamic processes [23-25]. It is also relatively difficult to experimentally investigate the reversibility of the pyrolysis reactions, while it may be one of the crucial steps for a better definition of the biomass pyrolysis reactions. However, recent findings in computational modelling stand as a great solution for the identification of these kinds of reaction mechanisms and validation of the modelling results with the experimental findings [26-29]. In previous studies, a group of different coal liquefaction mechanisms which consists of reversible and irreversible steps were suggested for a variety of different coals and the most promising liquefaction mechanisms were clarified and determined and clarified using the Kalman filter method, which is recently an attractive techniques used in chemical reactions, with the validation of experimental results [26-29].

The significance of this manuscript with respect to the understanding the pyrolysis mechanism and kinetics of four different biomass feedstocks (Asbos-Psilocaulon utile, Kraalbos-Galenia africane, Scholtzbos-Pteronia pallens, and Palm shell) using a novel filtering method; Kalman Filter. As this is the first study which demonstrate the applicability of Kalman Filter for the prediction of mechanisms and kinetics of the proposed biomass pyrolysis models. Based on this, five different generalised pyrolysis models consisting of reversible and irreversible were proposed to predict the pyrolysis mechanisms of these biomasses with Kalman Filter and Regression analysis. The validity of the proposed models is determined by the sum of the squared differences of the values calculated with the models and experimental data.

2. Experimental Method and Pyrolysis Models

2.1. Experimental data

The experimental biomass pyrolysis data which were used in the discrete-time models in this study had been produced by Jongh et al. [30] who investigated the vacuum pyrolysis of Asbos (Psilocaulon utile), Kraalbos (Galenia africane) and Scholtzbos (Pteronia pallens) at 450°C for 30, 60 and 90 mins, and by Abnisa et al. [31] who investigated the fast pyrolysis of Palm shell at 500°C for 30, 60, 90, 120 and 150 mins. The pyrolysis products (*i.e.* bio-char, bio-oil and gas) are presented in Appendix A Tab A1. These experimental data were used to validate the proposed models and investigate the pyrolysis kinetics by the application of Kalman filter and Regression analysis.

2.2. Proposed pyrolysis mechanisms

A variety of pyrolysis models consisting of series and parallel steps has been published to identify the biomass pyrolysis having different properties [32-34]. Five different biomass pyrolysis models based on lumped parameters of bio-oil (liquid, B) and gas (C) have been investigated for the pyrolysis of the four different biomasses feedstocks; Asbos (Psilocaulon utile), Kraalbos (Galenia africane) and Scholtzbos (Pteronia pallens), and Palm shell. The proposed biomass pyrolysis models have a group of parallel and series irreversible-reversible reaction steps, as shown in Fig 1. Model-1 illustrates a simplistic biomass pyrolysis mechanism involving the subsequent formation of liquid and gases from the thermal decomposition of biomass. Model-2 represents a reversible reaction between solid and liquid products in addition to the Model-1. Contrary to the first two models, Model-3 consists of two parallel irreversible reactions where the liquid and gas products are simultaneously produced from the biomass. Model-4 presents an additional pyrolysis step from liquid to gas products in addition to the proposed pyrolysis Model-3. In addition to irreversible pyrolysis steps, reversible reaction steps

by the polymerisation of liquid products thanks to the trace amount of transition metals may also occur. Therefore, Model-5 represents a reversible reaction between solid and liquid products in addition to the proposed pyrolysis models in Model-4. In the models, A, B, and C represent the remaining bio-char, bio-oil, and gas, respectively.

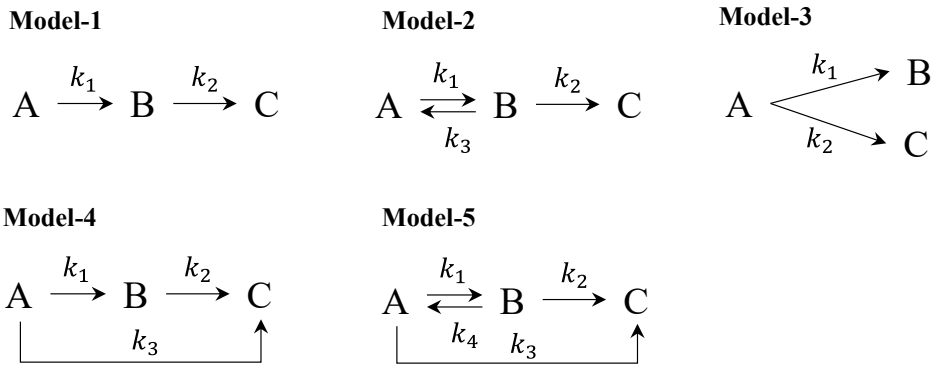

Figure 1. Proposed biomass pyrolysis models. A represents the biomass (or remaining char), B and C represent the pyrolysis products as bio-oil and gas, respectively.

The very early studies about biomass pyrolysis have been proposed that the decomposition rates of the biomass can be modelled based on the thermal behaviour of the main components and their relative contribution to the chemical structure of biomasses [35-38]. Biomasses can thermally decompose through the breaking of the chemical bonds in their molecules and produces a gas mixture rich in hydrocarbons, a bio-oil based liquid, and a solid (bio-char) rich in carbon (as shown in predicted models in Fig 1). The produced fragments usually become smaller molecules, however, they may also combine to produce a residue with a larger molecular mass, even amorphous covalent solids. Therefore, the yield of these products and pyrolysis mechanism mainly depends on the chemical composition of the raw biomass and the pyrolysis conditions such as temperature, heating rate, and residence time. Biomasses may contain water, oxygen, and/or other substances, which may contribute to combustion, hydrolysis, or any other chemical process besides pyrolysis [39]. However, the adverse chemical reactions may be avoided by the application of an inert atmosphere or vacuum conditions. Additionally, pyrolysis in a vacuum atmosphere may decrease the boiling point of the by-products, which improves their recovery [40, 41].

The current reaction steps accepted for the biomass pyrolysis assume that the volatiles (including some moisture) are evaporated below 100 °C [42]. Additionally, heat-sensitive substances such as proteins may partially decompose at this stage. When the pyrolysis temperature reaches around 100-120°C, the remaining moisture is removed from the material but higher temperatures are required to remove the water trapped in the crystal structure of hydrates. For example, sugars in the biomass structures start decomposition at 160-180 °C showing some condensable chemicals start decomposition in a very early stage of the pyrolysis, which provides by parallel pyrolysis mechanisms as suggested in Model 3-5 instead of series steps. Additionally, the organic molecules (fats, waxes, sugars etc.,) break down at a temperature between 100-500 °C [42]. Additionally, the main biomass structures such as hemicellulose, cellulose, and lignin also demonstrate thermal decomposition trends at about 220-315°C, 315-400°C, 160-900°C, respectively [43-45].

A large number of volatile organic compounds and non-condensable gases (H_2, CH_4, C_nH_m, CO, CO_2 and N) may release from the biomass processed by pyrolysis [46-48]. Some of the volatiles may ignite and burn to create a visible flame. The solid residue from the pyrolysis of the biomasses is generally described as "bio-char" having a rich carbon content with a colour ranging from brown to black. The char also consists of ash and a trace amount of contaminated metals such as Na, K, Hg, Cd, Be, Se, Sb, As, Pb, Zn, Cr, Co, Ni) [49-51], which may catalyse the pyrolysis reaction with an additional cracking reaction [52-54], which support a series reaction from bio-oil to gases as suggested in Model-1,2,4 and 5. On the other side, free radicals may polymerise and produce high molecule weight products [28, 29, 55] as suggested reversible steps in Model-2 and Model-5. As it is known that biomass-based waxes consist of a group of chemicals including n-alkanes, branched-chain alkanes, alkenes, esters, free fatty acids, primary and secondary fatty alcohols, aldehydes, ketones, and many others [53, 56]. In the presence of oxygen, some of the carbonaceous and nitrogen residues may oxidise at about 200-300 °C with no (or little) visible flame and thus the combustion gases CO, CO_2 and NOx are released [57]. Furthermore, the other elements such as Sulphur, Chlorine and Arsenic may also be oxidised at this stage.

2.3. Kalman filter method

Kalman filter, also known as linear quadratic estimation, is an iterative mathematical process, which uses a set of equations and consecutive data inputs to estimate the unknown variables in a process, which tends to be more precise than those based on a single measurement [58-61]. Kalman filter can be used to predict the unknown parameters using the known parameters of the period with the minimum variance of state variables; using three main stages of Filtering, Smoothing, and Prediction [60, 62]. The Kalman filter operates in two steps; first, estimate the current state of variables, along with their uncertainties in the prediction step. Second, once the output of the next measurement is obtained, these estimates are updated using a weighted average, with more weight being given to estimates with higher certainty [28]. Therefore, the reaction rate constants of the complex biomass pyrolysis models can be predicted using the Kalman filter method. Further information about the Kalman filtering theory and its application in the prediction of kinetic parameters of different chemical processes using Matlab has been presented in previous studies [26-29].

The compliance of the proposed pyrolysis models with the experimental data is figured out by forming first-order [63] linear discrete-time models [29, 55, 64]. Additionally, the reaction rate constants for each of the reactions in the models are determined using a Matlab programme (written in ver 7.11, The MathWorks Inc. Natick, MA, USA) with the use of the Kalman filter. The discrete-time models and reaction rate equations are provided in Eq 1-3 and Eq 4-6 as an example of Model-5. The reaction rate equations for the Models 1-4 are provided in Appendix B.

$$C_{A(i+1)} = C_{Ai}(1 - (k_1 + k_3)\Delta t) + k_4 C_{Bi}\Delta t \quad (1)$$

$$C_{B(i+1)} = C_{Bi} + (k_1 C_{Ai} - (k_2 + k_4)C_{Bi})\Delta t \quad (2)$$

$$C_{C(i+1)} = C_{Ci} + (k_3 C_{Ai} + k_2 C_{Bi})\Delta t \quad (3)$$

Where, C_A is unreacted biomass yield (wt.%), C_B and C_C are liquid and gas product yields (wt.%), respectively, k is the reaction rate constants for each reaction.

For Model-5

$$\frac{dA}{dt} = -(k_1 + k_3)A + k_4B \quad (4)$$

$$\frac{dB}{dt} = k_1A - (k_2 + k_4)B \quad (5)$$

$$\frac{dC}{dt} = k_2B + k_3A \quad (6)$$

2.4. Regression analysis method

Regression analysis is a method used to determine the relationship between at least two variables [65]. It is not only determines the model of the relationship between variables but also makes predictions for the unknown variable using the known variables and investigates the strength of the relationship between these variables [65-68]. In the regression analysis using the SigmaPlot (ver. 12.0 Notebook, Systat Software, Inc.) program, as the first step, the equation giving the lowest error rate with the experimental results for the biomasses is found in a cubic expression (Eq 8). The coefficients of Eq 8 were determined and presented in Appendix A Tab A2. The derivative of this equation gives the reaction rate equation (Eq 9). The reaction rate equations of Model-5 are presented in Eqs 10-12. The reaction rate equations for the Models 1-4 are provided in Appendix B. General regression equation;

$$y = a + bx \quad (7)$$

$$Y = y_0 + at + bt^2 + ct^3 \quad (8)$$

$$\frac{dY}{dt} = a + 2bt + 3ct^2 \quad (9)$$

Where y is the dependent variable, a, b and c are regression coefficients, x is the independent variable.

For Model 5

$$\frac{dA}{dt} = -k_1A^m - k_3A^n + k_4B^p \quad (10)$$

$$\frac{dB}{dt} = k_1A^m - k_2B^r - k_4B^p \quad (11)$$

$$\frac{dC}{dt} = k_3A^n + k_2B^r \quad (12)$$

The best model explaining the pyrolysis of selected biomasses is defined by the sum of the squared differences of the values calculated with the models and experimental data, using Eq 13 [28].

$$\sum_i \left(y_{m_i} - y_{e_i}\right)^2 = (l_m - l_e)^2 + (g_m - g_e)^2 \quad (13)$$

Where y_{m_i} and y_{e_i}; the values calculated from the model and the experimental data, l_m and l_e; the liquid yields g_m and g_e; the gas yields calculated using the model and the experimental data.

3. Results and Discussion

3.1. Determination of pyrolysis kinetics with Kalman filter

The findings from the models by forming first-order linear discrete-time models with the application of Kalman filter are compared with the experimental data supplied for Asbos (Psilocaulon utile), Kraalbos (Galenia africane) and Scholtzbos (Pteronia pallens), and Palm shell and the results are presented in Figs 2-6. Additionally, the reaction rate constants for each of the reactions in the proposed models and the sum of the squared differences of the values calculated with the models and experimental data are shown in Tab 1. In Model-1, the biomass is first converted to liquids (B), which can also be defined as bio-oil, and then gases (C) are produced from the bio-oils in a serial

reaction pathway. It is assumed that the pyrolysis of biomass would cause the scission of the bond in a specific way [55]. Therefore, first, a group of fragments, which is defined as liquid bio-oil, would be produced with the thermal decomposition of biomass. The other assumption in Model-1 is that the non-condensable gases (i.e. H_2, CH_4, CO, CO_2 and N) are formed by the thermal or catalytic cracking of the liquid bio-oil.

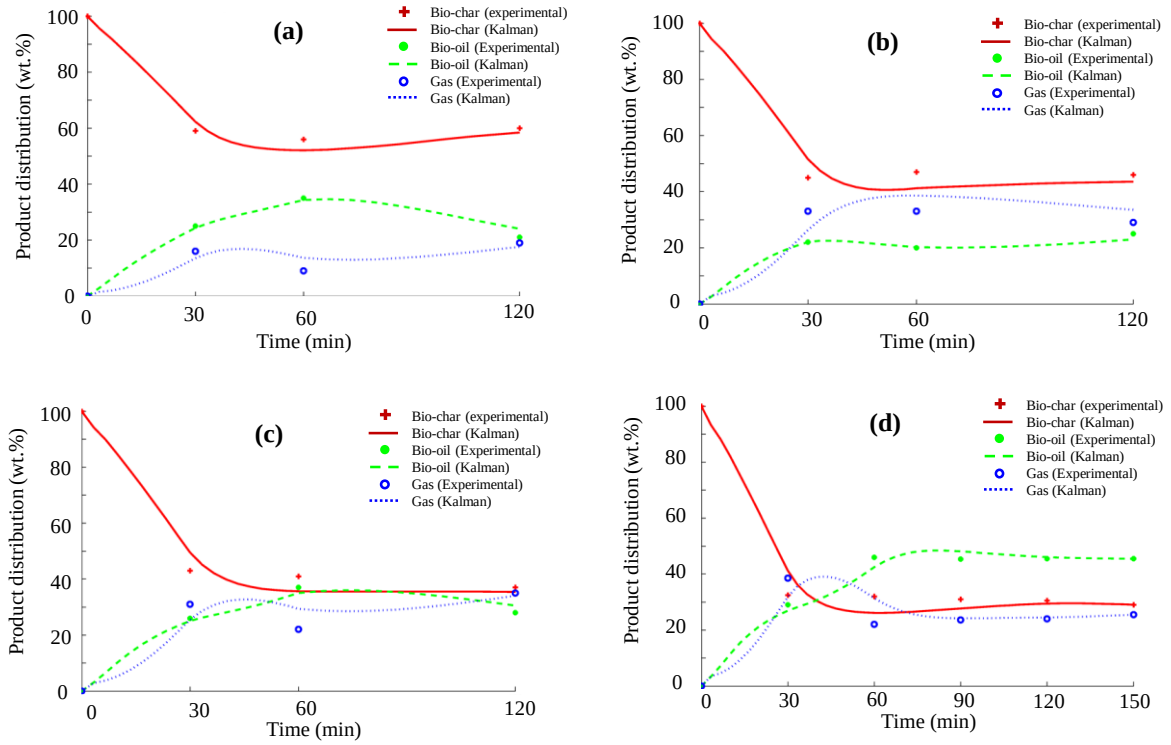

Figure 2. Comparison of Model-1 with the experimental data for a) Asbos (Psilocaulon utile), b) Scholtzbos (Pteronia pallens), c) Kraalbos (Galenia africane), and d) Palm shell.

In addition to Model-1, Model-2 represents a reversible reaction between bio-char ↔ bio-oils under the assumption of polymerisation of the free radicals in liquid products. The sum of square differences obtained by the comparison of Model-1 and Model-2 with the experimental data demonstrate that these models cannot fully describe the biomass pyrolysis, as demonstrated in Tab 1. The incompatibility of Model-1 (Fig 2) and Model-2 (Fig 3) with the experimental data prove that the gas products may arise from biomass rather than bio-oil.

The experimental results demonstrate that both gas and liquid yields were gradually increased in the first 30 min of the pyrolysis of Asbos (Psilocaulon utile), Scholtzbos (Pteronia pallens), Kraalbos (Galenia africane) and Palm shell. Therefore, the models having parallel pyrolysis reactions from biomass (A) to bio-oil (B) and gas (C) would be expected to demonstrate a better explanation for the pyrolysis of these biomasses as proposed in Model-3. Fig 4 (Model-3) shows the importance of the parallel reactions; biomass to bio-oil and biomass to gas, for the definition of the biomass pyrolysis as the model shows better fit with the experimental data compared with Model-1 and Model-2.

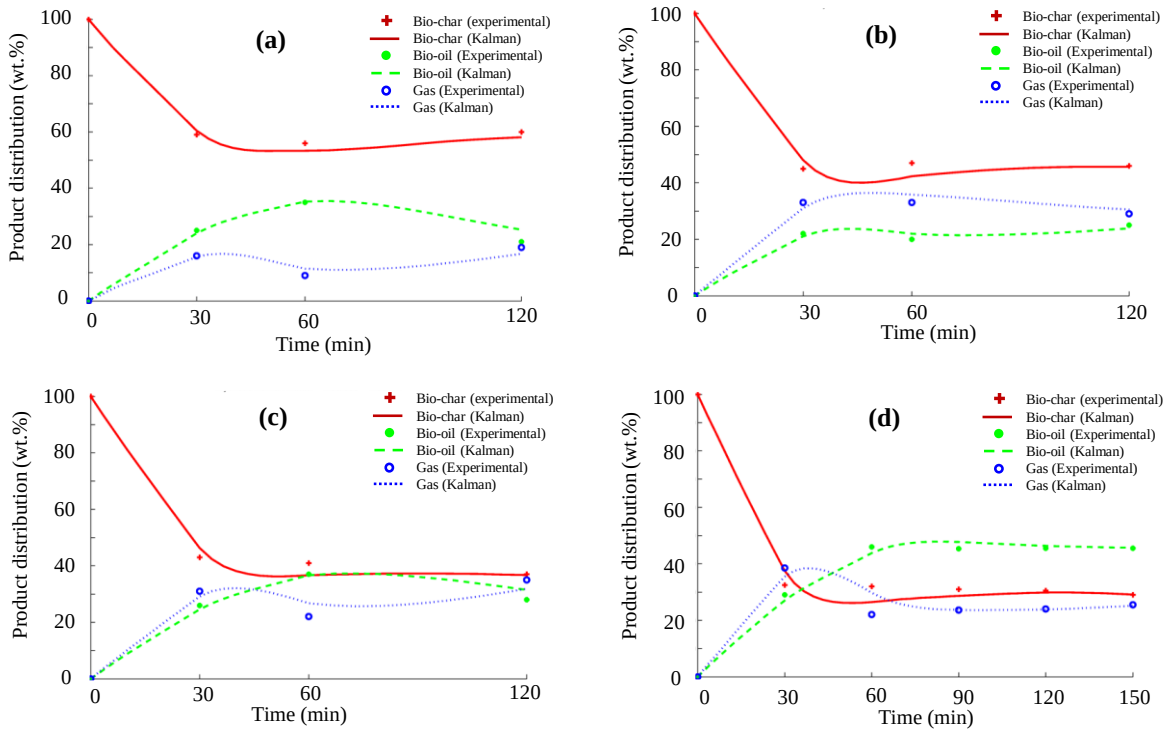

Figure 3. Comparison of Model-2 with the experimental data for a) Asbos (Psilocaulon utile), b) Scholtzbos (Pteronia pallens), c) Kraalbos (Galenia africane), and d) Palm shell.

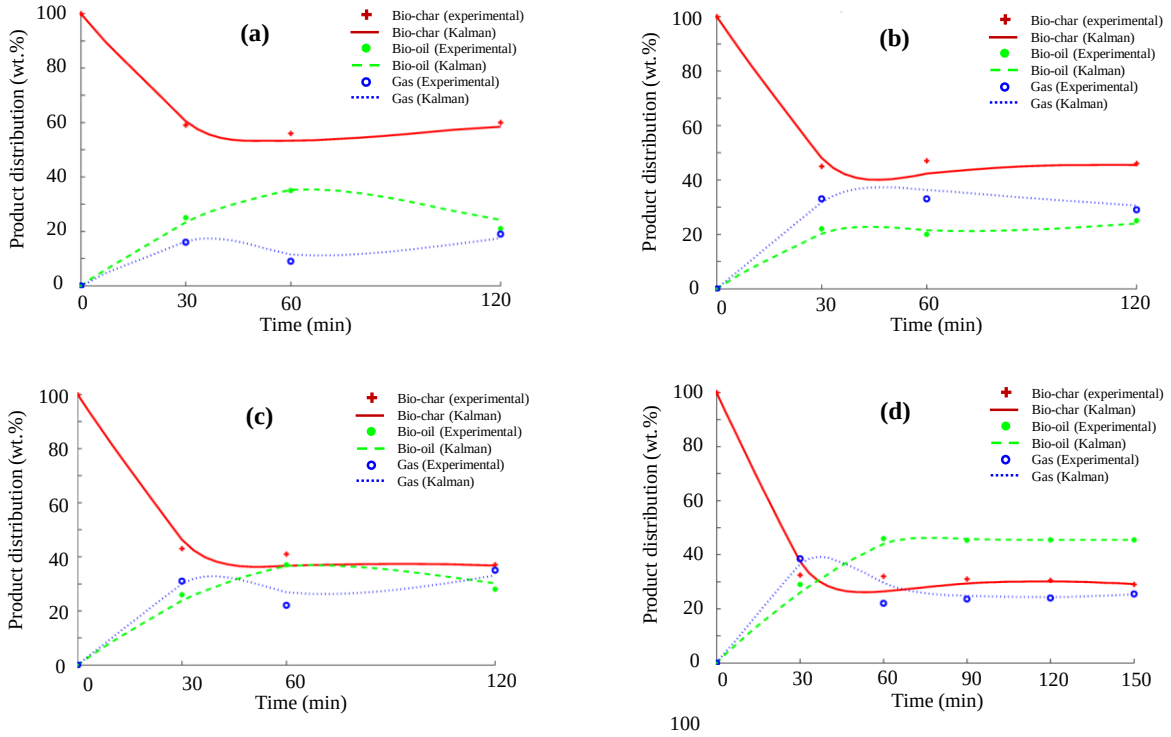

Figure 4. Comparison of Model-3 with the experimental data for a) Asbos (Psilocaulon utile), b) Scholtzbos (Pteronia pallens), c) Kraalbos (Galenia africane), and d) Palm shell.

In addition to these parallel reactions, the formation of gases may also be contributed by the cracking of bio-oils over the trace metals in the biomass. As metals such as Cu, Co, Mn and Fe may contribute to the pyrolysis reaction with cracking reactions [52, 54, 69]. The experimental data demonstrates

that although the formation of bio-oil continues to increase, the formation of gas slightly decreases after 60 min for the pyrolysis of Asbos (Psilocaulon utile) and Kraalbos (Galenia africane). Subsequently, a decrease in the bio-oil yield was observed after 120 min with an increase in gas and/or char yields. The increase in the gas yield may be attributed to the cracking of bio-oils by the catalytic effects of trace amount of metals. Therefore, the Model-3 is updated with an additional reaction step from bio-oil to gases, as presented in Model-4. Furthermore, the increase in bio-char may also be attributed to the polymerisation of free radicals. A large number of free radicals can be formed by the cracking of hydrocarbons thanks to the Beta scission reaction, which breaks the carbon-carbon bond. The free radicals may polymerise and produce high molecule weight products in the absence of hydrogen, which demonstrates an additional reversible reaction step between biomass ↔ bio-oils as presented in Model-5.

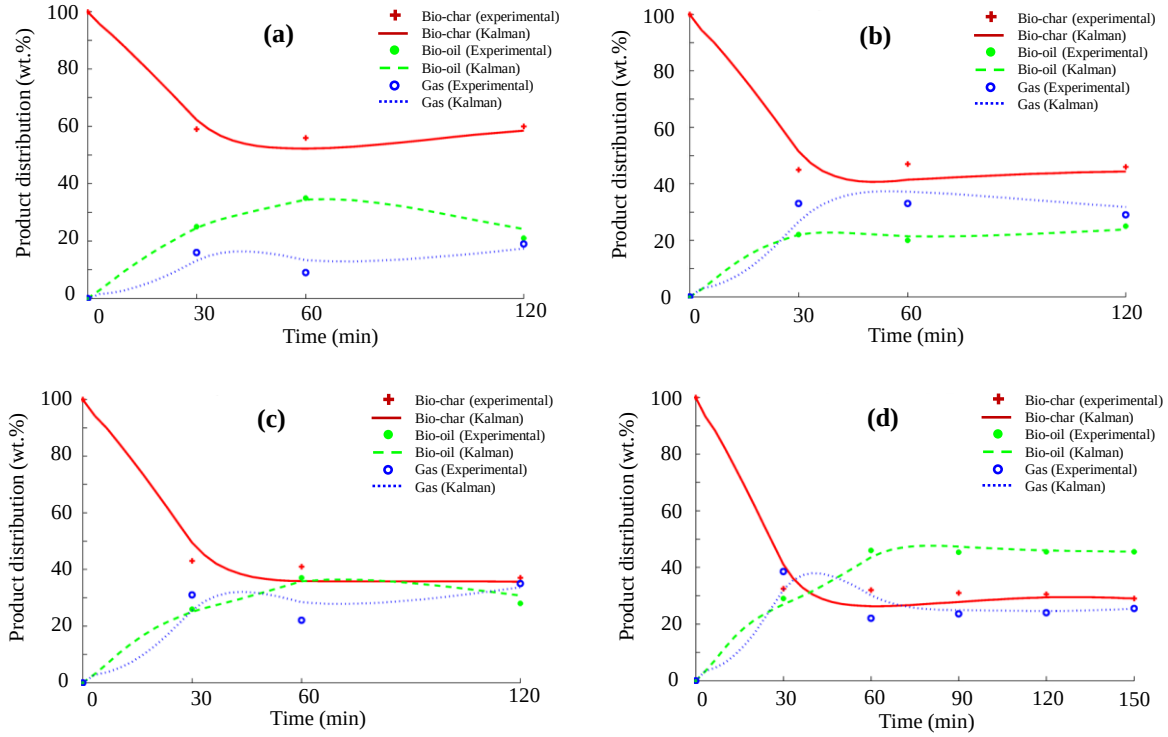

Figure 5. Comparison of Model-4 with the experimental data for a) Asbos (Psilocaulon utile), b) Scholtzbos (Pteronia pallens), c) Kraalbos (Galenia africane), and d) Palm shell.

As demonstrated in Fig 5 and Fig 6, the models; Model-4 and Model-5, in which the formation of bio-oil and gas products from direct biomass pyrolysis have a better fitting with the experimental data supplied from the pyrolysis of all four biomasses. Furthermore, the sum of the squared differences (Tab 1) supports this fitting and the importance of the reversibility between bio-char and bio-oil. Model-5 represents the best fitting with experimental data for the vacuum pyrolysis of Asbos (Psilocaulon utile), Scholtzbos (Pteronia pallens), Kraalbos (Galenia africane) compared with the other models, as shown in Fig 5. Model-4 demonstrates the best fitting with the experimental data for the fast pyrolysis of Palm shell compared with the other models, as demonstrated in Fig 6. Furthermore, the sum of the squared differences illustrated in Tab 1 also proves that Model-4 and Model-5 have the best prediction for biomass pyrolysis compare with the other three models.

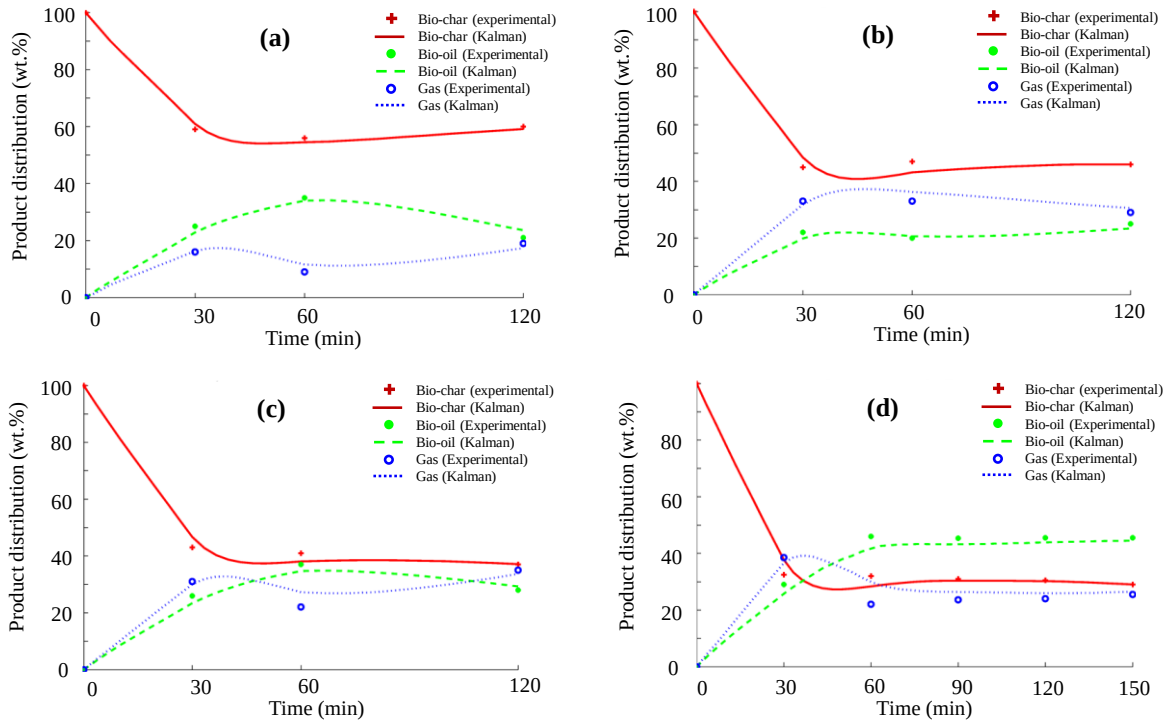

Figure 6. Comparison of Model-5 with the experimental data for a) Asbos (Psilocaulon utile), b) Scholtzbos (Pteronia pallens), c) Kraalbos (Galenia africane), and d) Palm shell.

Table 1. The sum of the squared differences of the values calculated with the models and experimental data for four different biomass and reaction rate constants (min^{-1}) for the models

Biomass	Models	$\sum_i (y_{m_i} - y_{e_i})^2$	Reaction rate constants (min^{-1})*10^3			
			k_1	k_2	k_3	k_4
Asbos (Psilocaulon utile)	Model 1	4.51	0.65	6.08	-	-
	Model 2	4.07	5.97	5.54	16.75	-
	Model 3	3.75	0.55	2.32	-	-
	Model 4	3.63	0.88	5.33	0.92	-
	Model 5	3.08	3.98	3.74	1.57	15.31
Scholtzbos (Pteronia pallens)	Model 1	6.65	3.95	8.07	-	-
	Model 2	6.36	11.26	7.60	16.09	-
	Model 3	4.56	1.28	0.14	-	-
	Model 4	4.37	1.68	0.09	0.01	-
	Model 5	3.98	8.21	0.38	0.32	16.15
Kraalbos (Galenia africane)	Model 1	7.07	4.98	8.67	-	-
	Model 2	6.88	15.83	7.59	14.86	-
	Model 3	4.06	0.95	3.62	-	-
	Model 4	4.17	0.50	5.29	2.01	-
	Model 5	3.85	9.34	1.73	6.04	15.38
Palm shell	Model 1	6.83	1.22	0.96	-	-
	Model 2	6.41	21.91	0.75	1.37	-
	Model 3	4.66	0.26	0.83	-	-
	Model 4	4.56	0.12	0.11	1.11	-
	Model 5	4.87	13.49	0.35	4.75	10.96

The kinetic results for Model-5 (Tab 1) demonstrate that the reaction rate from biomass → bio-oil (k_1) is much higher than the reaction rate from biomass → gas (k_3) for the pyrolysis of these biomasses. Similar to the experimental data in which the formation of bio-oil was faster than the formation of gas. As the highest reaction rate for the pyrolysis step of biomass → bio-oil for Asbos (Psilocaulon utile), Scholtzbos (Pteronia pallens), Kraalbos (Galenia africane) and Palm shell was determined as $3.9*10^{-3}$, $8.2*10^{-3}$, $9.3*10^{-3}$, and $13.5*10^{-3}$ min^{-1}, respectively. Furthermore, the reaction rate for the reversible step from bio-oil to bio-char (presented in Model-5) was found as $1.5*10^{-2}$ min^{-1} for the vacuum pyrolysis of Asbos (Psilocaulon utile), Scholtzbos (Pteronia pallens), Kraalbos (Galenia africane) and as $1.1*10^{-2}$ min^{-1} for the fast pyrolysis of Palm shell.

4.3. Determination of pyrolysis kinetics with Regression analysis

The reaction rates and orders were determined by regression analysis for the best three models defined by the Kalman filter, and the results are presented in Tab 2. Although Model 5 does not provide a better fit in the regression analysis, Model 3 and Model 4 were presented a relatively low sum of the squared differences with the experimental data collected by the vacuum pyrolysis of Asbos, Scholtzbos, Kraalbos, and fast pyrolysis of Palm shell. The reaction rate from biomass → bio-oil (k_1) and biomass → gas (k_3) were calculated much higher than the reaction rate from bio-oil → gas (k_2) in Model 4. This may be attributed to the formation of gas run through direct biomass pyrolysis with a small contribution by bio-oil cracking as the reaction order (p) for this step was also much lower than the other pyrolysis steps, as presented in Tab 2. On the other side, the relatively high reaction order for the main pyrolysis steps (from biomass to bio-oil or gas) was determined as presented in Tab 2. The variety of the reaction orders has resulted from the differences in the biomass. In Model 3, the reaction orders for the pyrolysis step from biomass → gas (n) were determined about 3.5 for Kraalbos, 2.8 for Scholtzbos and 2.2. for Palmshell, which are roughly 1.6-1.1 times higher than the pyrolysis step from biomass → bio-oil (m).

Table 2. The sum of the squared differences of the values calculated with the models and experimental data for four different biomass and reaction rate constants (mass fraction$^{(1-n)}$ min^{-1}) for the models.

Biomass / **Models**	$\sum_i (y_{m_i} - y_{e_i})^2$	Reaction rate constants (mass fraction$^{(1-n)}$ min^{-1})				Reaction orders			
		k_1	k_2	k_3	k_4	m	n	p	r
Asbos (Psilocaulon utile)									
Model 3	6.74	$1.2*10^{-8}$	$1.2*10^{-7}$	-	-	4.0	3.4	-	-
Model 4	6.71	$6.9*10^{-10}$	$7.6*10^{-17}$	$1.2*10^{-7}$	-	4.6	3.4	0.6	-
Model 5	49.53	$2.4*10^{-26}$	$2.0*10^{-2}$	$1.6*10^{-7}$	$8.6*10^{-3}$	1.6	1.7	1.3	0
Scholtzbos (Pteronia pallens)									
Model 3	13.03	$9.7*10^{-6}$	$3.4*10^{-6}$	-	-	2.5	2.8	-	-
Model 4	13.17	$7.1*10^{-2}$	$5.1*10^{-17}$	$3.4*10^{-6}$	-	0.6	2.8	0	-
Model 5	13.17	$7.1*10^{-2}$	$3.5*10^{-18}$	$3.4*10^{-6}$	$9.5*10^{-16}$	0.6	2.8	0	0
Kraalbos (Galenia africane)									
Model 3	22.30	$5.7*10^{-5}$	$1.6*10^{-7}$	-	-	2.2	3.5	-	-
Model 4	23.12	$3.6*10^{-1}$	$6.6*10^{-24}$	$7.5*10^{-7}$	-	0.2	3.2	0.4	-
Model 5	1000<	$3.2*10^{-1}$	$1.0*10^{-17}$	$1.6*10^{-7}$	$4.5*10^{-6}$	1.6	3.5	1.3	0.6
Palm shell									
Model 3	14.80	$5.0*10^{-4}$	$5.4*10^{-5}$	-	-	1.7	2.2	-	-
Model 4	14.68	$4.8*10^{-5}$	$4.4*10^{-20}$	$5.5*10^{-5}$	-	2.3	2.2	0	-
Model 5	1000<	$3.5*10^{-1}$	$2.7*10^{-16}$	$5.4*10^{-5}$	$3.0*10^{-4}$	2.2	0	2.2	0

Conclusion

The models, Model-3, Model-4, and Model-5, where the products are formed from biomass in parallel pyrolysis reactions show a better fit with the experimental data compared with Model-1 and Model 2, proposing pyrolysis in a series of reactions by Kalman filter and Regression analysis. However, the Kalman filter provided a better estimation for the biomass pyrolysis reaction kinetics compared to regression analysis. Model-5 was the best-proposed models, which consists of reversible reaction steps in addition to parallel pyrolysis steps with the assumption of first-order linear discrete-time models. The highest reaction rate for the pyrolysis of Asbos, Scholtzbos, Kraalbos, and Palm shell was found as $3.9*10^{-3}$, $8.2*10^{-3}$, $9.3*10^{-3}$, and $13.5*10^{-3}$ min^{-1}, respectively, for the step from biomass $\rightarrow$ bio-oil. Although it is possible to generalise, the reaction rate constants and reaction orders are fully dependent on the biomass properties.

This study demonstrates that the Kalman filter is a promising filtering method to estimate the biomass pyrolysis models and parameters using minimum experimental data as the most stable results were obtained with the Kalman filter. As future work, detailed biomass pyrolysis mechanisms to value-added chemicals (products) could be investigated to identify the impact of pyrolysis conditions such as residence time, temperature, and heating rate in a commercial pyrolysis process. Those detailed pyrolysis mechanisms must be investigated for specific type of biomass due to the differences in physicochemical properties of biomass feedstocks.

Symbols

a, b, c	-	regression coefficients in regression analysis
C_A	[wt.%]	unreacted biomass yield
C_B	[wt.%]	liquid product yields
C_C	[wt.%]	gas product yields (wt.%)
g_m	[wt.%]	gas yields determined by model
g_e	[wt.%]	experimental gas yields
l_m	[wt.%]	liquid yield determined by model
l_e	[wt.%]	experimental liquid yield
k_1 to k_4	[min^{-1}]	reaction rate constants
y	-	dependent variable in regression analysis
y_{mi}	[wt.%]	values calculated from the model data in the sum of the squared differences
y_{ei}	[wt.%]	values calculated from the experimental data in the sum of the squared differences
x	-	independent variable in regression analysis

Subscripts

A	Biomass
B	Liquid products from pyrolysis
C	Gas products from pyrolysis
e	Experimental data
m	Model data

References

[1]. M. Kumar, A. O. Oyedun, A. Kumar, *Renew. Sustain. Energy Rev* **2018**, 81, 1742-1770. DOI: 10.1016/j.rser.2017.05.270

[2]. E. T. Kostas, O. S. Williams, G. Duran-Jimenez, A. J. Tapper, M. Cooper, R. Meehan, J. P. Robinson, *Biomass Bioenergy* **2019**, 125, 41-49. DOI: 10.1016/j.biombioe.2019.04.006

[3]. K. Tekin, S. Karagöz, S. Bektaş, *Renew. Sustain. Energy Rev* **2014**, 40, 673-687. DOI: 10.1016/j.rser.2014.07.216

[4]. F. Gulec, E.H. Simsek, A. Karaduman, A. *J. Fac. Eng. Archit. Gazi Univ* **2016**, 313, 610-621. DOI: 10.17341/gummfd.93160
[5]. F. Güleç, L.M.G. Riesco, O. Williams, E. T. Kostas, A. Samson, and E. Lester, *Fuel* **2021**, 302, 121166. DOI: 10.1016/j.fuel.2021.121166
[6]. Y. Shen, *Biomass Bioenergy* **2020**, 134. DOI: 10.1016/j.biombioe.2020.105479
[7]. G. Özsin, A. E. Pütün, E. Pütün, *Biomass Convers. Biorefin* **2019**, 9 (3), 593-608. DOI: 10.1007/s13399-019-00390-9
[8]. Q. Zhang, J. Chang, T. Wang, Y. Xu, *Energy Convers. Manag* **2007**, 48 (1), 87-92. DOI: 10.1016/j.enconman.2006.05.010
[9]. S. Hameed, A. Sharma, V. Pareek, H. Wu, Y. Yu, *Biomass Bioenergy* **2019**, 123, 104-122. DOI: 10.1016/j.biombioe.2019.02.008
[10]. N. Khuenkaeo, S. Phromphithak, T. Onsree, S. R. Naqvi, N. Tippayawong, PloS one 16, no. 7 (2021): e0254485. doi.org/10.1371/journal.pone.0254485
[11]. P. Basu, Biomass gasification, pyrolysis and torrefaction: practical design and theory, Academic press, 2018.
[12]. I. Ali, R. Tariq, S. R. Naqvi, A. H. Khoja, M. T. Mehran, M. Naqvi, N. Gao, *J. Energy Inst.* **2021**, 95, 30-40. DOI:10.1016/j.joei.2020.12.002.
[13]. S. A. Khan, I. Ali, S. R. Naqvi, K. Li, M. T. Mehran, A. H. Khoja, A. A. Alarabi, A. Atabani, *J Anal Appl Pyrolysis* **2021**, 105149. DOI:10.1016/j.jaap.2021.105149.
[14]. N. Prakash, T. Karunanithi, J. Appl. Sci. R*es.* **2008**, 4 (12), 1627-1636.
[15]. N. Prakash, T. Karunanithi, *Asian J. Sci. Res.* **2009**, 1, 1-27.
[16]. M. J. Antal, G. Varhegyi, E. Jakab, *Ind. Eng. Chem* **1998**, 37 (4), 1267-1275. DOI: 10.1021/ie970144v
[17]. D. S. Scott, J. Piskorz, D. Radlein, *Ind. Eng. Chem. Process*. **1985**, 24 (3), 581-588.
[18]. F. Thurner, U. Mann, *Ind. Eng. Chem. Process.* **1981**, 20 (3), 482-488.
[19]. G. Varhegyi, M. J. Antal Jr, E. Jakab, P. Szabó, *J Anal Appl Pyrolysis* **1997**, 42 (1), 73-87.
[20]. P.N. Sheth, B.V. Babu, *Proceedings of national conference on environmental conservation* **2006**, 453-458.
[21]. E. Ranzi, A. Cuoci, T. Faravelli, A. Frassoldati, G. Migliavacca, S. Pierucci, S. Sommariva, *Energy Fuels* **2008**, 22 (6), 4292-4300. DOI: 10.1021/ef800551t
[22]. A. Cuoci, T. Faravelli, A. Frassoldati, S. Granata, G. Migliavacca, S. Pierucci, E. Ranzi, S. Sommariva, In Proceedings of the 30th Meeting on Combustion *CELL* **2007**, 531 (303), 445.
[23]. C. Boztepe, A. Künkül, N. Gürbüz, and I. Özdemir, *Int. J. Chem* **2019**, 51,12, 931-942. DOI: 10.1002/kin.21321
[24]. C. Boztepe, A. Künkül, N. Gürbüz. *J. Mol. Struct.* **2020**, 1209, 127948. DOI: 10.1016/j.molstruc.2020.127948
[25]. C. Boztepe, M. Daskin, A. Erdogan, T. Sarici, *Polym. Eng. Sci.* **2021**, 61, 2083–2096. DOI: 10.1002/pen.25736
[26]. G. B. Greg Welch, University of North Carolina at Chapel Hill, 2006, 16.
[27]. M. Grewal, A. Andrews. Kalman filtering: theory and practice using MATLAB, John Wiley, New York, 2001.
[28]. E. H. Şimşek, F. Güleç, H. Kavuştu, *Fuel* **2017**, 207, 814-820. DOI: 10.1016/j.fuel.2017.06.004
[29]. E. H. Şimşek, F. Güleç, H. Kavuştu, A. Karaduman, *J. Fac. Eng. Archit. Gazi Univ* **2019**, 34 (1), 79-88. DOI:10.17341/gazimmfd.416464
[30]. W. A. De Jongh, M. Carrier, J. H. Knoetze, *J Anal Appl Pyrolysis* **2011**, 92 (1), 184-193. DOI: 10.1016/j.jaap.2011.05.015
[31]. F. Abnisa, W. W. Daud, W. Husin, J. Sahu, *Biomass Bioenergy* **2011**, 35 (5), 1863-1872. DOI: 10.1016/j.biombioe.2011.01.033
[32]. A. Anca-Couce, *Prog. Energy Combust.* **2016**, 53, 41-79. DOI: 10.1016/j.pecs.2015.10.002
[33]. J. Blondeau, H. Jeanmart, *Biomass Bioenergy* **2012**, 41, 107-121. DOI: 10.1016/j.biombioe.2012.02.016
[34]. A. Sharma, V. Pareek, D. Zhang, *Renew. Sustain. Energy Rev* **2015**, 50, 1081-1096. DOI: 10.1016/j.rser.2015.04.193
[35]. S. Ward, J. Braslaw, *Combust. Flame* **1985**, 61 (3), 261-269. DOI: 10.1016/0010-2180(85)90107-5
[36]. C. Koufopanos, A. Lucchesi, G. Maschio, *Can J Chem Eng* 1989, 67 (1), 75-84. DOI: 10.1002/cjce.5450670111
[37]. P. T. Williams, S. Besler, *Fuel* **1993**, 72 (2), 151-159. DOI: 10.1016/0016-2361(93)90391-E
[38]. J. Caballero, R. Font, A. Marcilla, *Thermochim. Acta* **1996**, 276, 57-77. DOI: 10.1016/0040-6031(95)02794-7
[39]. M. Balat, M. Balat, E. Kırtay, H. Balat, *Energy Convers. Manag.* **2009**, 50 (12), 3147-3157. DOI: 10.1016/j.enconman.2009.08.014
[40]. M. Garcìa-Pèrez, A. Chaala, C. Roy, *J Anal Appl Pyrolysis* **2002**, 65 (2), 111-136. DOI: 10.1016/S0165-2370(01)00184-X
[41]. M. Garcia-Perez, A. Chaala, H. Pakdel, D. Kretschmer, C. Roy, *J Anal Appl Pyrolysis* **2007**, 78 (1), 104-116. DOI: 10.1016/j.jaap.2006.05.003
[42]. H. Zhou, Y. Long, A. Meng, Q. Li, Y. Zhang, *Thermochim. Acta* **2013**, 566, 36-43. DOI: 10.1016/j.tca.2013.04.040
[43]. M. Carrier, L. Auret, A. Bridgwater, J. H. Knoetze, *Energy Fuels* **2016**, 30 (10), 7834-7841. DOI: 10.1021/acs.energyfuels.6b00794
[44]. H. Yang, R. Yan, H. Chen, D. H. Lee, C. Zheng, *Fuel* **2007**, 86(11-12), 1781-1788. DOI: 10.1016/j.fuel.2006.12.013
[45]. H. Zhou, Y. Long, A. Meng, S. Chen, Q. Li, Y. Zhang, *Rsc Adv* **2015**, 5 (34), 26509-26516. DOI: 10.1039/C5RA02715B

[46]. F. Pinto, F. Paradela, F. Carvalheiro, L. C. Duarte, P. Costa, R. N. André, *Chem. Eng. Trans.* **2018**, 70, 793-798. DOI: 10.3303/CET1870133
[47]. M. N. Uddin, W. W. Daud, H. F. Abbas, *Renew. Sustain. Energy Rev* **2013**, 27, 204-224. DOI: 10.1016/j.rser.2013.06.031
[48]. M. Shahbaz, A. AlNouss, P. Parthasarathy, A. H. Abdelaal, H. Mackey, G. McKay, T. Al-Ansari, *Biomass Conv. Bioref.* **2020**, 1-13. DOI: 10.1007/s13399-020-01040-1
[49]. Q. Qi, C. Sun, J. Zhang, Y. He, Y. W. Tong, *Chem. Eng. J* **2021**, 406, 126833. DOI: 10.1016/j.cej.2020.126833
[50]. L. Abou Jaoude, P. Castaldi, N. Nassif, M. V. Pinna, G. Garau, *Sci. Total Environ* **2020**, 711, 134511. DOI: 10.1016/j.scitotenv.2019.134511
[51]. J. Tang, C. Cao, F. Gao, W. Wang, *Environ. Technol. Innov* **2019**, 16, 100492. DOI: 10.1016/j.eti.2019.100492
[52]. F. Güleç, W. Meredith, C.-G. Sun, C. E. Snape, *Energy* **2019**, 173, 658-666. DOI: 10.1016/j.energy.2019.02.099
[53]. T. Ahmad, M. Rafatullah, A. Ghazali, O. Sulaiman, R. Hashim, *J Environ Sci Health C* 2011, 29 (3), 177-222. DOI: 10.1080/10590501.2011.601847
[54]. F. Güleç, W. Meredith, C.-G. Sun, C. E. Snape, *Chem. Eng. J* **2020**, 389, 124492. DOI: 10.1016/j.cej.2020.124492
[55]. E. H. Simsek, F. Güleç, F. S. Akcadag, *Fuel Process. Technol* **2020**, 198, 106227. DOI: 10.1016/j.fuproc.2019.106227
[56]. E. H. Sin, The extraction and fractionation of waxes from biomass, University of York 2012.
[57]. H. Chen, Y. Wang, G. Xu, K. Yoshikawa, *Energies* **2012**, 5 (12), 5418-5438. DOI: 10.3390/en5125418
[58]. R. E. Kalman, *J. Basic Eng.* **1960**, 82, 1, 35-45.
[59]. G. Welch, G. Bishop, Department of Computer Science University of North Carolina at Chapel Hill Chapel Hill, NC, 1995, 27599-3175.
[60]. R. J. Meinhold, N. D. Singpurwalla, *Am Stat* **1983**, 37 (2), 123-127.
[61]. E.A. Wan, R. Van Der Merwe, In Proceedings of the IEEE **2000** Adaptive Systems for Signal Processing, Communications, and Control Symposium (Cat. No. 00EX373), IEEE, **2000**, 153-158.
[62]. S.J. Julier, J.K. Uhlmann, In Signal processing, sensor fusion, and target recognition VI, **1997**, 3068, 182-193.
[63]. G. Varhegyi, E. Jakab, M. J. Antal Jr, *Energy Fuels* **1994**, 8 (6), 1345-1352.
[64]. F. Güleç, and G.D.T. Ozdemir, *Akademik Ziraat Dergisi* **2017**, 6(1), 73-80.
[65]. M. P. Allen, Understanding regression analysis, Springer Science & Business Media, 2004.
[66]. C. Lu, W. Song, W. Lin, *Biotechnol Adv* **2009**, 27 (5), 583-587. DOI: 10.1016/j.biotechadv.2009.04.014
[67]. S. Chatterjee, A. S. Hadi, Regression analysis by example, John Wiley & Sons, 2015.
[68]. D. C. Montgomery, E. A. Peck, G. G. Vining, Introduction to linear regression analysis, John Wiley & Sons, 2021.
[69]. F. Güleç, W. Meredith, C.-G. Sun, C. E. Snape, *Fuel* **2019**, 244, 140-150. DOI: 10.1016/j.fuel.2019.01.168

Table and Figure Captions

Table 1. The sum of the squared differences of the values calculated with the models and experimental data for four different biomass and reaction rate constants (min^{-1}) for the models

Table 2. The sum of the squared differences of the values calculated with the models and experimental data for four different biomass and reaction rate constants (mass fraction$^{(1-n)}$ min^{-1}) for the models.

Figure 1. Proposed biomass pyrolysis models. A represents the biomass (or remaining char), B and C represent the pyrolysis products as bio-oil and gas, respectively.

Figure 2. Comparison of Model-1 with the experimental data for a) Asbos (Psilocaulon utile), b) Scholtzbos (Pteronia pallens), c) Kraalbos (Galenia africane), and d) Palm shell.

Figure 3. Comparison of Model-2 with the experimental data for a) Asbos (Psilocaulon utile), b) Scholtzbos (Pteronia pallens), c) Kraalbos (Galenia africane), and d) Palm shell.

Figure 4. Comparison of Model-3 with the experimental data for a) Asbos (Psilocaulon utile), b) Scholtzbos (Pteronia pallens), c) Kraalbos (Galenia africane), and d) Palm shell.

Figure 5. Comparison of Model-4 with the experimental data for a) Asbos (Psilocaulon utile), b) Scholtzbos (Pteronia pallens), c) Kraalbos (Galenia africane), and d) Palm shell.

Figure 6. Comparison of Model-5 with the experimental data for a) Asbos (Psilocaulon utile), b) Scholtzbos (Pteronia pallens), c) Kraalbos (Galenia africane), and d) Palm shell.

Table of Contents:

The significance of this research with respect to the understanding the pyrolysis mechanism and kinetics of four different biomass feedstocks using a novel filtering method; Kalman Filter. As this

study demonstrates that Kalman Filter is a promising method for the prediction of biomass pyrolysis mechanisms and kinetics.

Graphical Abstract: